ARF Binds the C-Terminal Region of the *Escherichia coli* Heat-Labile Toxin (LTA_1) and Competes for the Binding of LTA_2

Xinjun Zhu,[‡] Elma Kim,[‡] Annette L. Boman,[‡,§] Alec Hodel,[‡] Witold Cieplak,[||] and Richard A. Kahn*[,‡]

Department of Biochemistry, Emory University School of Medicine, 1510 Clifton Road, Atlanta, Georgia 30322-3050, and Ribi Immunochem Research, Inc., 553 Old Corvallis Road, Hamilton, Montana 59840

Received November 15, 2000; Revised Manuscript Received January 3, 2001

ABSTRACT: Cholera toxin (CT) and the heat-labile enterotoxin (LT) from *Escherichia coli* are highly related in terms of structure and biochemical activities and are the causative agents of cholera and traveler's diarrhea, respectively. The pathophysiological action of these toxins requires their activity as ADP-ribosyltransferases, transferring the ADP-ribose moiety from NAD onto the stimulatory, regulatory component of adenylyl cyclase, Gs. This reaction is highly dependent on the protein cofactor, termed ADP-ribosylation factor (ARF), that is itself a 20 kDa regulatory GTPase. In this study, we define sites of interaction between LTA and human ARF3. The residues identified as important to ARF binding include several of those previously shown to bind to the A2 subunit of the toxin and those important to the organization of two flexible loops, previously implicated as regulators of substrate entry. A model for how ARF acts to enhance the catalytic activity is proposed. A critical portion of the overlap between ARF and LTA_2 in binding LTA_1 includes a short region of sequence homology between LTA_2 and the switch II region of ARF. LTA_2 also interacted with ARF effectors in two-hybrid assays, and thus, we discuss the possibility that the LTA_2 subunit may function in cells as a partial ARF mimetic to compete for the binding of ARF to LTA_1 or regulate aspects of the toxin's transport from the cell surface to the ER.

Cholera toxin (CT)[1] and the heat-labile enterotoxin from *Escherichia coli* (LT) are potent, causative agents for diarrheal diseases (*1*, *2*) whose sequences are ~80% identical and whose three-dimensional structures (*3*−*6*) and modes of action are almost identical. The intracellular target of both toxins is Gs, the stimulatory regulatory component of adenylyl cyclase (*7*−*9*). LT and CT are hexameric AB-type toxins with five identical B subunits and one catalytic A subunit (*10*). The B pentamer binds cell surface GM_1 gangliosides (*11*) to initiate the internalization and processing of the toxin by eukaryotic cells. LTA is made up of 240 residues and is processed to LTA_1 (residues 1−192) and LTA_2 (residues 193−240) by sequential amide and disulfide bond cleavage reactions. The enzymatic (ADP-ribosyltransferase) activity of the toxins is located in the A_1 subunit of the toxins (*12*), and in cells results in the ADP-ribosylation of Gsα, the loss of GTPase activity, and the consequent persistent activation of adenylyl cyclase (*7*). The resulting increase in cyclic AMP levels in cells leads to the massive loss of fluids and ions from cells lining the gastrointestinal tract that characterize these pathological states (*1*).

The LTA_2 subunit is comprised of an extended α-helix that lies along one surface of LTA_1 and the more flexible C-terminus that binds to the B pentamer to link the A and B subunits together. The presence at the C-terminus of a KDEL sequence, a signal for retrieval to the ER, is important to the localization and efficient processing of the toxin through the retrograde vesicular transport (*10*, *13*, *14*).

The in vitro ADP-ribosyltransferase activity of the bacterial toxins is highly dependent on a protein cofactor, termed ADP ribosylation factor (ARF) (*15*, *16*), that belongs to the superfamily of regulatory GTPases. In addition to cofactor activity for the bacterial toxins, ARFs are implicated as regulators of a number of cellular reactions and processes, including activators of phospholipase D (*17*, *18*) and phosphatidylinositol 4-phosphate 5-kinase (*19*, *20*) activities and control of vesicular membrane traffic, principally between the ER and Golgi (*21*−*23*) but also other membrane sites (*24*−*27*). The structures of ARF with either GDP or GTP bound have been determined and are very similar to those of Ras (*28*, *29*). These GTPases have two mobile loops, termed switch I and switch II, that become ordered upon binding GTP and which are involved in the binding of effectors or other proteins (*30*, *31*). The direct interaction between LTA and ARF has been demonstrated both by the robust stimulation of ADP-ribosyltransferase activity using purified components (*15*) and by the recent demonstration

* To whom all correspondence should be addressed. Phone: (404) 727-3561. Fax: (404) 727-3746. E-mail: rkahn@emory.edu.

[‡] Emory University School of Medicine.

[§] Current address: Department of Biochemistry and Molecular Biochemistry, University of Minnesota−Duluth, Duluth, MN 55812.

[||] Ribi Immunochem Research, Inc.

[1] Abbreviations: AD, activation domain of GAL4 used in fusion proteins in two-hybrid assays; ARF, ADP-ribosylation factor; BD, DNA binding domain of GAL4 used in fusion proteins in two-hybrid assays; CT, cholera toxin; LT, heat-labile enterotoxin from *E. coli*; LTA, subunit of LT that contains the catalytic and linker functions; LTA_1, catalytic subunit of LTA consisting of the first 192 residues of LTA; LTA_2, linker region of LTA (residues 193−240) that links LTA_1 to the B pentamer; LTB, subunit of LT that binds to membrane receptors as a pentamer and also to the C-terminus of LTA.

10.1021/bi002628s CCC: $20.00
Published on Web 03/22/2001

that LTA increases the GTP binding affinity for ARF (*32*). The binding of activated (GTP-bound) ARF to LTA is reported to lower the binding constants for substrates, NAD^+ and Gsα (*33*).

The NAD^+ binding site has been well characterized as it is conserved among a large number of NAD^+ binding proteins (*34*−*37*). From models of the structure of LT and mutants, it has been predicted that activation involves the sequential coordination of conformational changes from the C-terminal region of LTA that propagate through a flexible loop (residues 25−36) to affect the catalytic site (*38*). LT and CT have ADP-ribosyltransferase or NADase (when water is the acceptor) activities that are not dependent on ARF and thus allow detailed structural studies in the absence of the protein cofactor. As a result, few studies have even addressed the question of where ARF binds or how it affects catalysis.

The structure of a RAS−RAS GAP($p120^{GAP}$) complex has been determined (*39*) by X-ray crystallography. The RAS binding surface is comprised of three α-helices and a flexible finger loop. These helices form the bottom of a shallow groove on the surface of the Ras GAP($p120^{GAP}$). The flexible finger loop contains the catalytic Arg^{789} residue that assists in the activation of the catalytic water involved in hydrolysis of the γ-phosphate of the RAS-bound GTP. Visual inspection revealed homology between the structure of the RAS-binding surface of Ras GAP($p120^{GAP}$) and the C-terminal region of LTA_1. This C-terminal region also contains several α-helices forming a shallow groove. In addition, the most flexible loop (residues 25−36) of LTA_1 also protrudes toward the surface of the C-terminal groove and contains a central Arg^{33} residue. These similarities led us to predict that the binding of LTA and ARF may be similar to that of the RAS−RAS GAP-($p120^{GAP}$) complex, even though no ARF GAP activity has been reported or was found for LTA (unpublished observation).

In addition to providing a better understanding of the evolutionary and functional relationship between endogenous factors and the bacterial toxins, the detailed elucidation of ARF−toxin binding also allows the production of toxins with specific defects in ARF binding that are ideal for future studies of LTA function and localization in mammalian cells and as a novel approach to the construction of toxin mutants as mucosal adjuvants with decreased toxicity. Indeed, a required role for ARFs in the pathophysiology of either toxin has not yet been demonstrated, in large part due to the ubiquity of ARFs in eukaryotes. LT and CT have each been shown to possess potent mucosal adjuvant activities (*40*, *41*). The need for ADP-ribosyltransferase activity for potent adjuvant activity has been reported (*42*), though it remains controversial (*43*). The toxicity resulting from ADP-ribosylation of cellular protein targets has limited the utility and development of these toxins as adjuvants. A toxin deficient in ARF binding but with retention of basal ADP-ribosyltransferase activity offers an alternative approach to the production of adjuvants with decreased toxicity. Thus, we took advantage of the interaction between activated ARFs and LTA in two-hybrid assays to design a loss-of-binding screen to rapidly identify residues that are critical to the interaction. We conclude that ARF interacts with LTA_1 through the nucleotide-sensitive switch I and switch II loops and that LTA_1 binds ARF via many of the same residues that bind LTA_2, including the C-terminal domain and flexible loop (residues 25−36) of LTA_1. The similarities between LTA_2 and ARF were found to extend to local sequence homology with potential importance to the trafficking and toxicity of these bacterial toxins.

MATERIALS AND METHODS

Materials. Nitrocellulose membranes were purchased from Schleicher & Schuell. All other standard reagents used in the formulation of assay solutions were obtained from Sigma. Radiolabeled nucleotides were purchased from New England Nuclear.

Reverse Two-Hybrid System and Gain-of-Interaction Two-Hybrid System. LTA and LTA mutants were engineered into the pACT2 vector for expression in yeast of a fusion protein with the GAL4 activation domain at the N-terminus, followed by the HA epitope (*44*). [Q71L]ARF3 was subcloned into pBG4D for expression of active ARF fused at the C-terminus to the GAL4 DNA-binding domain and HA tag to create plasmid pAB304 (*45*). LTB was subcloned into the pAS1-CYH vector for expression of the LTB subunit fused to the GAL4 binding domain at its N-terminus. Random mutagenesis of the open reading frame of [E112D]LTA in addition to 130 base pairs at each end was performed by PCR under conditions of reduced stringency, as described previously (*46*, *47*). A gapped pACT2 plasmid was made by digestion with *Nco*I and *Bam*HI and purification. The mutagenized PCR product and the gapped plasmid were transformed into yeast Y190 strain *MAT a gal4 gal80 his3 trp1-901 ade 2-101 ura3-52 leu2-3, 112 URA3::GAL*-lacZ, LYS2::GAL(UAS)-HIS3 cyh^r (a gift from S. Elledge) already carrying pAB304 to create strain YAB457. Transformants grew up within 3 days before being transferred onto nitrocellulose membranes and testing by the β-galactosidase assay (*48*). Colonies that were white or light blue were selected and checked for the expression of full-length LTA by immunoblotting, using 12CA5 monoclonal antibody against the HA tag. The full-length LTA mutants were then tested for retention of LTB binding in two-hybrid assays. Those mutants that retained interaction with LTB were sequenced for identification of mutations. When screening for gain-of-interaction LTA mutants, we used the same method as described, except that the parent strain carried a double mutation in ARF3, either [V53M/Q71L]ARF3 or [Q71L/I74S]ARF3, rather than [Q71L]-ARF3. When screening for ARF mutants that lost interaction with [E112D]LTA, we used the same method described above except the PCR mutagenesis was performed on the open reading frame of [Q71L]ARF3.

Expression and Purification of Recombinant ARF Mutants. ARF mutants were subcloned into bacterial expression vector pET3C (*49*−*51*) for expression in bacteria, using *Nde*I and *Bam*HI sites. These mutants were then transformed into BL21(DE3) cells for recombinant protein expression, purification, and determination of guanine nucleotide binding properties, as described previously (*52*, *53*).

Expression and Purification of Recombinant LT Subunits. LTA was expressed in bacteria and purified as described by Cieplak et al. (*57*). LTA_2 was subcloned into the bacterial expression vector pET28 (Invitrogen) at the *Bam*HI site. The resulting plasmid was transformed into BL21(DE3) cells for recombinant protein expression and purification on a 1 mL

high trap chelation column charged with Ni (Pharmacia) and then on a 200 mL Superdex 75 column.

Liquid β-Galactosidase Assay. β-Galactosidase activity was quantified from liquid yeast cultures using the method of Guarente et al. (*54*). Duplicates of yeast strains were grown in 5 mL of minimal (SD) selective medium overnight at 30 °C. The next day, 5 mL of fresh selective medium was inoculated with 20−50 μL of the overnight culture and cultured to mid-log phase, $2-5 \times 10^7$ cells/mL (OD_{600} = 0.3−0.7). Cells were collected by centrifugation and resuspended in 1 mL of Z buffer (40 mM Na_2HPO_4, 40 mM NaH_2PO_4, 10 mM KCl, and 1 mM Mg_2SO_4 (pH 7.0)) and put on ice. Cells (50 and 100 μL) were mixed with Z buffer to a volume of 1 mL, and 1 drop of 0.1% SDS and 2 drops of chloroform were added to each sample using a Pasteur pipet. The mixtures were vortexed for 10−15 s and equilibrated for 15 min at 30 °C. *O*-Nitrophenol α-D-galactopyranoside (ONPG, 0.8 mg) was added, and the solution was vortexed for 5 s and incubated at 30 °C until a medium-yellow color had developed in the positive controls. The reaction was stopped by adding 0.5 mL of 1 M Na_2CO_3, and the time was recorded. OD_{420} and OD_{550} were determined after the cell debris was removed by centrifugation. Units of β-galactosidase activity were determined using the equation $U = 1000(OD_{420} - OD_{550})/(TVOD_{600})$, where *V* is the volume of the culture used in the assay (microliters), *T* is the time of reaction (minutes), OD_{600} is the cell density at the start of the assay, OD_{420} represents the combination of absorbance by ONPG and light scattering by cell debris, and OD_{550} represents the light scattering by cell debris.

NAD−Agmatine ADP-Ribosyltransferase Assay. LTA was activated by incubation at 30 °C for 10 min in buffer containing 50 mM glycine (pH 8.0) and 20 mM dithiothreitol with trypsin (type I from bovine pancreas; Sigma Chemical Co.) at a ratio of 15:1 (LTA to trypsin). The reaction was stopped by the addition of a 1-fold molar excess of soybean trypsin inhibitor (type I-S; Sigma Chemical Co.). Reactions were performed as previously described (*55*), and the mixtures contained 50 mM potassium phosphate (pH 7.5), 4 mM NAD (6 nM [*adenine*-2,8-^{3}H]NAD), 10 mM agmatine, 20 mM dithiothreitol, 2 mM $MgCl_2$, 100 μM GTPγS, 3 mM DMPC, 0.1% cholate, 0.1 mg/mL BSA, 1 μM ARF, and 4 μM LTA in Figure 1. Reactions were initiated by the addition of the LTA, and after a 90 min incubation at 30 °C, duplicate 0.1 mL samples were loaded onto 2 mL Dowex AG 1-X2 columns to separate the product, ADP-ribosylagmatine, from the NAD. When the ARF-dependent activity was determined (e.g., Figure 1), the activity seen in the absence of ARF was subtracted from those samples containing ARF.

RESULTS

Deletion of C-Terminal Helices or Mutations in the Flexible Finger Loop Resulted in the Loss of Interaction with ARF. The complete LTA subunit is comprised of LTA_1 (residues 1−192) and LTA_2 (residues 193−240). The latter provides a link between the catalytic A_1 subunit and the B pentamer. We have recently described the use of two-hybrid assays with C-terminal fusion proteins of human ARF proteins to identify and modulate ARF binding proteins and effectors (*45*, *47*, *56*). The [Q71L]ARF3 mutant is deficient in GTP hydrolysis and is a dominant activator of ARF activities in cells, allowing a selection for proteins that interact preferentially with the activated, GTP-bound form of the GTPase. To test the prediction that the C-terminal region of LTA_1 is involved in ARF binding, we first deleted the A_2 subunit to generate N-terminal fusion proteins with the GAL4 transcriptional activation domain ([E112D]LTA_1-AD) for use in two-hybrid assays of protein interactions (Table 1). Because the wild-type LTA and LTA_1 toxins were found to be toxic to yeast, leading to slow cell growth, this and later LTA_1 constructs contained the E112D mutation that has previously been shown to decrease ADP-ribosyltransferase activity to less than 10% of that of the wild-type protein (*57*), without altering the interaction with ARF (*58*). As shown in Table 1, the ability to bind [Q71L]ARF3 was undiminished by the introduction of the E112D mutation into LTA or by the deletion of the A_2 subunit from [E112D]-LTA to yield [E112D]LTA_1. LTA_1 has previously been shown to be fully active in ADP-ribosyltransferase assays (*33*, *58*, *59*) and effects on GTPγS binding to ARF (*32*) assays and thus contains a fully functional ARF binding site.

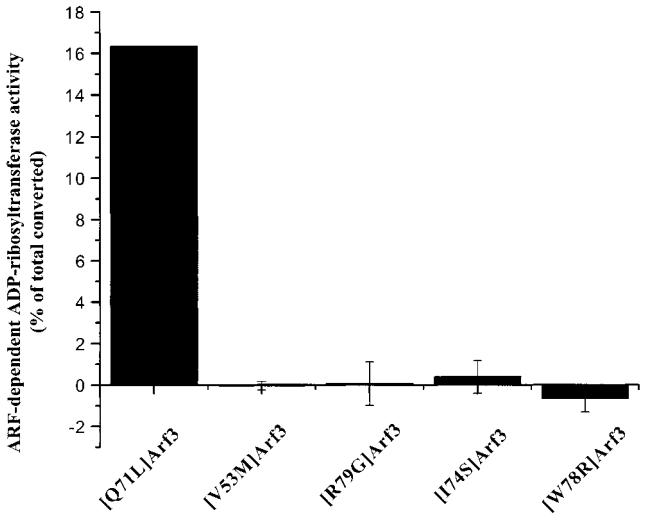

FIGURE 1: Loss-of-interaction mutants of ARF3 have also lost the ability to activate LTA in the ADP-ribosyltransferase assay. LTA was preactivated by incubation at 30 °C for 10 min in buffer containing 50 mM glycine (pH 8.0) and 20 mM dithiothreitol. The activated LTA (4 μM) was then added to the ADP-ribosylation assay, with different mutants of ARF3 (1 μM), as described in Materials and Methods. The activity present in the absence of ARF was subtracted to determine the ARF-dependent activity and is expressed as the percentage of substrate converted to product. The specific activity in the absence of ARF was 5.06 pmol of ADP-ribosylated agmatine formed per minute per microgram of LTA in the experiment shown. The averages of triplicate determinations are shown with error bars representing the standard error of the mean. This experiment was repeated at least twice.

We tested the importance of the α-helices and the flexible loop of [E112D]LTA_1 to ARF binding by generating additional mutations in the [E112D]LTA_1-AD construct and assaying its ability to bind to ARF in yeast two-hybrid assays. Deletions of either the two (α8 and α9) or three (α7−α9) short α-helices at the C-terminus caused the loss of all interaction with [Q71L]ARF3 (see Table 1). Similarly, the point mutation of Arg^{33} to Ala^{33} in the flexible loop of [E112D]LTA_1 led to the loss of interaction with [Q71L]-ARF3-BD. Two other point mutations in the finger loop were made to test the involvement of those residues in ARF binding. Mutation of Phe^{31} to Leu^{31} caused loss of interaction

Table 1: Deletions at the C-Terminus or Mutations within the Flexible Loop of LTA_1 Lose the Ability To Bind [Q71L]ARF3[a]

LTA protein	[Q71L]ARF3	LTB
LTA	+++	+
[E112D]LTA	+++	+
[E112D]LTA_1	+++	−
[E112D/Δ173−192]LTA_1	−	−
[E112D/Δ155−192]LTA_1	−	−
[F31L/E112D]LTA	−	+
[D32H/E112D]LTA	+++	+
[R33A/E112D]LTA	−	+

[a] The left column shows the mutation(s) in LTA; the middle column shows results of two-hybrid assays of each LTA when paired with the activated [Q71L]ARF3, and the right column shows the activity in two-hybrid assays when paired with LTB. LTA constructs in diploid yeast strains were tested for their ability to interact with [Q71L]ARF3 and LTB using the filter-bound β-galactosidase assay, as described in Materials and Methods. The symbol +++ indicates a strong blue color developed within 15 min of addition of the substrate to the β-galactosidase assay; a single plus sign (+) indicates activity seen within 6 h, and a hyphen (−) represents no visible color development after overnight (16 h) incubation at 30 °C. The [E112D/Δ173−192]LTA_1 or [E112D/Δ155−192]LTA_1 mutant represents a deletion of C-terminal α-helices 8 and 9 or α-helices 7−9, respectively. Note that neither the introduction of the E112D mutation nor the deletion of the LTA_2 subunit interfered with the binding of ARF3.

with [Q71L]ARF3. In contrast, mutation of Asp^{32} to His^{32} had no effect and the loop retained full binding to [Q71L]-ARF3. The presence of the α-helices at the C-terminus and flexibility of the loop are predictive of minimal disturbance in the folding and stability of the [E112D]LTA_1 protein by these mutations. This was supported by experimental evidence which showed that each of these mutants was soluble and expressed in yeast to approximately the same level, as determined by immunoblots using the monoclonal anti-HA antibody, 12CA5. These data supported our prediction that the finger loop, and specifically Arg^{33} and Phe^{31}, and the C-terminal helices of LTA_1 are involved in the binding of ARF.

Screening for Loss-of-Interaction Mutants of LTA_1 with the Yeast Two-Hybrid Assay. To obtain a more complete model of the binding surface between LTA and ARF, we screened for mutations in [E112D]LTA that had lost the ability to bind to [Q71L]ARF3. The "reverse two-hybrid" system that was used involved PCR mutagenesis of the [E112D]LTA open reading frame and selection for white colonies with the β-galactosidase screen for interactions, as described in Materials and Methods. Full-length, stable LTA mutants were selected by counterscreening after pairing with the B subunit (LTB-BD) in two-hybrid assays and by immunoblotting yeast extracts using the 12CA5 antibody that reacts with the HA epitope at the C-terminus of the [E112D]-LTA-AD-HA fusion proteins. Plasmids expressing full-length LTA mutants that no longer interacted with [Q71L]ARF3-BD were rescued from yeast and were retested after fresh transformations. The coding regions of [E112D]LTA were then sequenced to identify any additional mutations, and the results are shown in Table 2.

Three additional mutations in [E112D]LTA that resulted in the loss of [Q71L]ARF3 binding were found from the reverse two-hybrid screen (see Table 2). Trp^{179}, changed to Arg^{179}, lies in α-helix 8 very near the C-terminus of LTA_1 and a cluster of hydrophobic residues previously identified as being critical to the stability of this region of the protein and to LTA activity (*60*). Asn^{93}, changed to Ile^{93}, is located at the surface of a loop between β-strand 5 and α-helix 4. Asp^{43} is in α-helix 2, was found mutated to Gly^{43}, and is also located near the C-terminus of LTA_1 in the folded protein (*10*). In this structure, Asp^{43} forms a hydrogen bond with Asn^{40} which may be important to the structure of the flexible loop carrying the essential Arg^{33}. Alternatively, the introduction of a glycine into the α-helix immediately downstream of the flexible loop and near the C-terminus may disrupt the helix and lead to a local loss of organization in this functionally critical region.

LTA Binding Domains on ARF. To investigate the regions of ARF involved in binding to LTA, we used the same strategy described above for LTA, a reverse two-hybrid screen for identifying mutants of [Q71L]ARF3 that decrease or lose altogether the interaction with [E112D]LTA. Instead of counterscreening with the LTB subunit, we used other ARF binding partners [e.g., MKLP1 (*45*); see Table 3]. Though several ARF mutants, such as [Q71L/I74S]ARF3, did not interact with ARF binding partners, we tested their binding abilities for GTP and/or GDP as described later to confirm that the mutant ARFs were folding properly and capable of specific, high-affinity interactions. Ten point mutants in ARF were identified in this way, and eight of these were located in switch I or switch II, the flexible loops whose structure are most dramatically impacted by the exchange of GDP for GTP (*31*). We selected five of these for more detailed analysis. ARF mutants were expressed in bacteria, and the purified proteins were characterized with respect to guanine nucleotide binding as additional proof of retention of overall folding. Each of these ARF mutants bound both GDP and GTPγS at a level within 2-fold (50−200%) of that of the parental [Q71L]ARF3. Three of the mutants, [V53M/Q71L]ARF3, [Q71L/I74S]ARF3, and [Q71L/R79G]ARF3, showed the same binding capacity for GTPγS as [Q71L]ARF3. The level of equilibrium binding of GTPγS to [V56A/Q71L]ARF3 or [Q71L/W78R]ARF3 was lower (50%) than that to [Q71L]ARF3. Thus, LTA resembles other ARF effectors in that residues in the two nucleotide sensitive switches are critical to binding.

Loss-of-Interaction Mutations in [Q71L]ARF3 Also Lack the Ability To Stimulate ADP-Ribosyltransferase Activity of LTA. We next investigated the abilities of the mutant ARFs to increase the ADP ribosyltransferase activity of LTA, as described in Materials and Methods. Four ARF3 mutants were employed and found to have lost the ability to stimulate the ADP-ribosyltransferase activity of LTA (see Figure 1). In contrast, [Q71L]ARF3 increased ADP ribosyltransferase activity to more than double that of ARF3 (not shown) (*32*).

Screening for Gain-of-Interaction Mutants. While the loss of a specific, high-affinity interaction surface can arise from either local or more general changes in protein structure, we reasoned that a gain-of-function mutation may be more likely to result from a local change in the binding site. Thus, to further investigate the ARF binding sites of LTA, we again mutagenized the [E112D]LTA open reading frame but this time selected for gain of interactions with one of two ARF3 double mutants that had lost binding to [E112D]LTA: one in switch I and one from switch II. [V53M/Q71L]ARF3 or [Q71L/I74S]ARF3 was used as bait in two-hybrid screens for [E112D]LTA second-site mutations that regained the ability to bind these ARFs. [E112D]LTA was mutagenized

Table 2: Summary of the Additional [E112D]LTA Mutants, Their Origin, Their Location in the Structure of LT (*10*), and the Consequences of the Binding of [Q71L]ARF3

mutation	origin	location	consequence
F31L	site-directed mutagenesis	flexible loop	loss of [Q71L]ARF3 binding
D32H	site-directed mutagenesis	flexible loop	no effect
R33A	site-directed mutagenesis	flexible loop	loss of [Q71L]ARF3 binding
D43G	reverse two-hybrid assay	α-helix linking loop and C-terminus	loss of [Q71L]ARF3 binding
N93I	reverse two-hybrid assay	loop under A_2	loss of [Q71L]ARF3 binding
Y145H	gain-of-interaction screen	α6	loss of [Q71L]ARF3 binding; gain of [Q71L]-, [V53M]-, or [I74S]ARF3 binding
Y149C	gain-of-interaction screen	α6	loss of [Q71L]ARF3 binding; gain of [Q71L]-, [V53M]-, or [I74S]ARF3 binding
L164F	gain-of-interaction screen	α7	loss of [Q71L]ARF3 binding; gain of [Q71L/I74S]ARF3 binding
W179R	reverse two-hybrid assay	α8, C-terminus	loss of [Q71L]ARF3 binding

Table 3: Mutations of Residues in Switches I and II of ARF3 Lead to Loss of [E112D]LTA Binding[a]

ARF3 protein	[E112D]LTA	MKLP1
[Q71L]ARF3	+++	+++
[L37R/Q71L]ARF3	−	+++
[V53M/Q71L]ARF3	−	++
[V56A/Q71L]ARF3	+	+
[V56G/Q71L]ARF3	−	−
[Y58C/Q71L]ARF3	+	+++
[I74S/Q71L]ARF3	−	−
[W78R/Q71L]ARF3	−	−
[R79G/Q71L]ARF3	+	+++

[a] Mutants of [Q71L]ARF3 with reduced ability or inability to bind [E112D]LTA were tested for their interaction with another ARF binding partner, MKLP1. Diploid yeast strains carrying both a [Q71L]ARF3 mutant and an ARF effector were assayed for β-galactosidase activity, as described in Materials and Methods. The symbols +, ++, and +++ represent increasing levels of activity, visualized and scored by eye as the intensity of blue product formation, while a hyphen (−) indicates no activity in a 60 min assay.

by PCR and ARF binding assayed using the β-galactosidase filter screen, as described in Materials and Methods. Because the protein is required for the gain of function, we did not need to counterscreen to ensure expression of full-length proteins, but we did counterscreen and select for mutants that did not bind the single ARF mutant, [Q71L]ARF3. The screen with [V53M/Q71L]ARF3 led to the isolation of [E112D/Y145H]LTA and [E112D/Y149C]LTA. Each of these residues lies in an α-helix, distal to the surface of the region of LTA_1 on which A_2 lies (see Figure 2). Tyr^{149}, in particular, makes close contacts with Lys^{217} in a region of LTA_2 that is homologous to switch II of ARF (see below). The screen with [Q71L/I74S]ARF3 also identified the same two mutants but found changes to two different residues: Tyr^{149} to His (twice) or Asn (once). In addition, two independently isolated mutations result in a change of Leu^{164} to Phe^{164}. Leu^{164} also lies along the surface of LTA_1 in which side chains bind to LTA_2, and in this case, it is much closer to the C-terminus of LTA_1 and the N-terminus of LTA_2 (see Figure 2). Together, the mutants identified from screens involving random mutagenesis implicate one surface of the LTA_1 structure as the ARF binding region, the same surface along which the A_2 subunit lies.

Homology between LTA_2 and Switch II of ARF. With cleavage of the amide bond after residue 192, the LTA_1 and LTA_2 subunits are held together by disulfide bonds between Cys^{187} and Cys^{199} and a series on interactions between the side chains of the long α-helix of LTA_2 with those residues

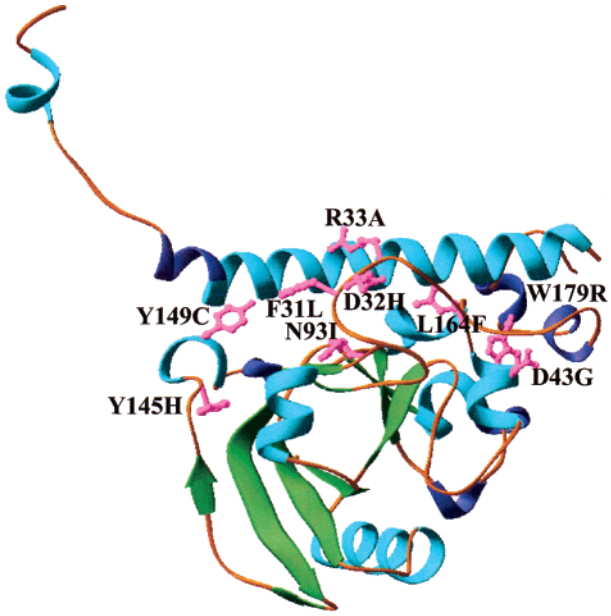

FIGURE 2: Ribbon drawing showing the mutations in LTA that were found to impact the binding of ARF3. Note that all mutations lie at the C-terminal region of LTA_1 and the flexible finger loop (residues 25−36), and that the side chains form the interface between subunits A_1 and A_2. In contrast, the silent mutation D32H points in the opposite direction.

lying along one surface of LTA_1 (see Figure 2). Because many of the same residues are involved in LTA_1 binding ARF and LTA_2, we looked for any sequence or structural homologies between the two LTA_1 binding partners.

A short region of homology was observed in LTA_2, at the site closest to the flexible loop of LTA_1 (residues 25−36), and in switch II of ARF3:

LTA_2: $Q^{215}S^{216}K^{217}V^{218}K^{219}$

ARF3: $Q^{71}D^{72}K^{73}I^{74}K^{75}$

in which a line indicates identity and a dotted line represents a conservative substitution. Given the previously determined importance of the flexible loop and this surface of the LTA_1 molecule to ARF binding and the role of switch II in ARF effector binding, we hypothesized that LTA_2 and ARF may interact with LTA_1 in similar ways and that LTA_2 may possess some ARF-mimetic activities beyond the simple binding to LTA_1. To test this model, we assayed the ability of LTA_2 to bind to other ARF effectors, besides LTA_1.

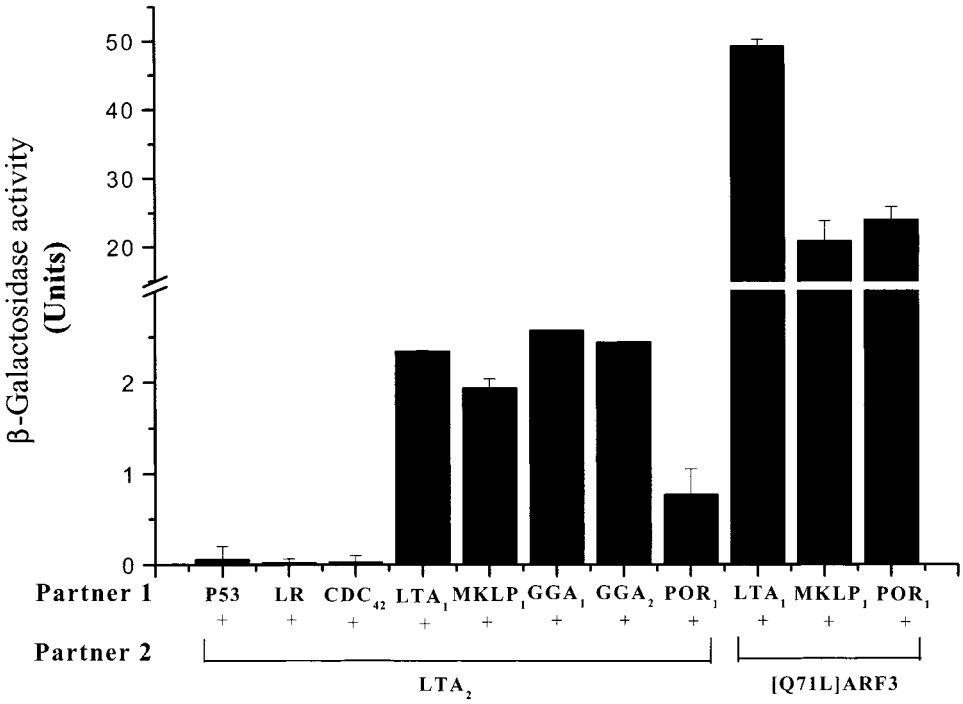

FIGURE 3: LTA_2 weakly, but specifically, interacts with ARF effectors in two-hybrid assays. LTA_2 was tested for its interaction with ARF partners, including [E112D]LTA_1, MKLP1, GGA1, GGA2, and POR1ΔN. Extracts from diploid yeast strains, each of which carried both LTA_2 and an effector or an unrelated protein [p53, lamin receptor (LR), or CDC42 was used as a negative control], were assayed for β-galactosidase activity using ONPG as a substrate, as described in Materials and Methods. Note the difference in scale between the activity observed between LTA_2 with ARF effectors and that of [Q71L]ARF3 with the same effectors.

Because [Q71L]ARF3 has been used successfully to identify novel binding partners using the same two-hybrid assays described above, we asked if LTA_2 bound those same ARF effectors. This was originally done using the filter lift assay that uses X-gal as the substrate and later using the solution-based, quantifiable assay that uses ONPG as the substrate. These two assays gave qualitatively identical results. We found that LTA_2 interacted specifically with each ARF effector but with none of the controls (unrelated proteins; see Figure 3). Not surprisingly, LTA_2 gave a much lower (10−20-fold) activity than did [Q71L]ARF3 with these same effectors (note the differences in the *y*-axis).

Because of similarities between the binding of ARF3 and LTA_2 to LTA_1 and the availability of previously identified mutants of LTA_1 with a decreased level of binding to activated ARF3, we asked if the same mutants lost binding to LTA_2. As seen in Table 4, two of the mutants of LTA_1 that had lost binding to [Q71L]ARF3 retained undiminished binding to LTA_2, as did the mutation (D32H) in the flexible loop that retained full binding to [Q71L]ARF3. In this way, we were able to distinguish between the binding of ARF3 and LTA_2 to LTA_1. We conclude from these results that the binding sites on LTA_1 for ARF3 and LTA_2 are similar but not identical.

LTA_2 Competes for the Binding of ARF3 to LTA_1. A prediction from the model in which the binding sites for ARF3 and LTA_2 overlap on the surface of LTA_1 is that each should compete for the binding of the other. Thus, a more stringent test was devised to determine if the presence of LTA_2 can inhibit activation of LTA_1 activity by ARF in the ADP-ribosyltransferase assay. We purified LTA_2 from bacteria and looked for changes in the amount of ARF-stimulated activity of LTA_1. As shown in Figure 4, we found that basal ADP-ribosyltransferase activity of LTA_1 was not influenced by the addition of an excess of LTA_2, but the ARF-stimulated activity could be suppressed to basal levels by the A_2 subunit, partially inhibited by LTA_2 protein, which further supported our model (see Figure 4).

Table 4: Mutations in LTA_1 That Eliminate Binding to [Q71L]ARF3 Have No Effect on the Binding of LTA_2[a]

LTA protein	binding to [Q71L]ARF3-BD	binding to LTA_2-BD
[E112D]LTA_1	+++	+
[E112D/F31L]LTA_1	−	+
[E112D/D32H]LTA_1	+++	+
[E112D/N93I]LTA_1	−	+

[a] The E112D and double-mutant LTA_1 were subcloned into the pACT2 vector for expression in yeast as N-terminal fusions with the activation domain of GAL4. The LTA_1 mutants were expressed in yeast with either[Q71L]ARF3-BD or LTA_2-BD fusion proteins and assayed for interactions using the filter-bound assay for β-galactosidase activity, using X-gal as a substrate. Activity was scored visually and rated as (−) no blue color development within 180 min, (+) blue color developing after only 60 min, and (+++) blue color apparent within less than 10 min of the assay at 30 °C, as described in Materials and Methods.

DISCUSSION

Two different random screens and a set of designed mutations all identified residues along one surface of LTA_1 that are involved in the binding of ARF and contribute to our conclusion that ARF binds to the same surface on LTA_1 along which LTA_2 lies in the holotoxin. We propose that upon binding, ARF is positioned to orient the hydrophobic region involving residues at the C-terminus of LTA_1 and two flexible loops to open the substrate binding sites and thereby lower the K_M for each substrate. We also conclude that the nucleotide sensitive "switch II" of ARF is involved in binding

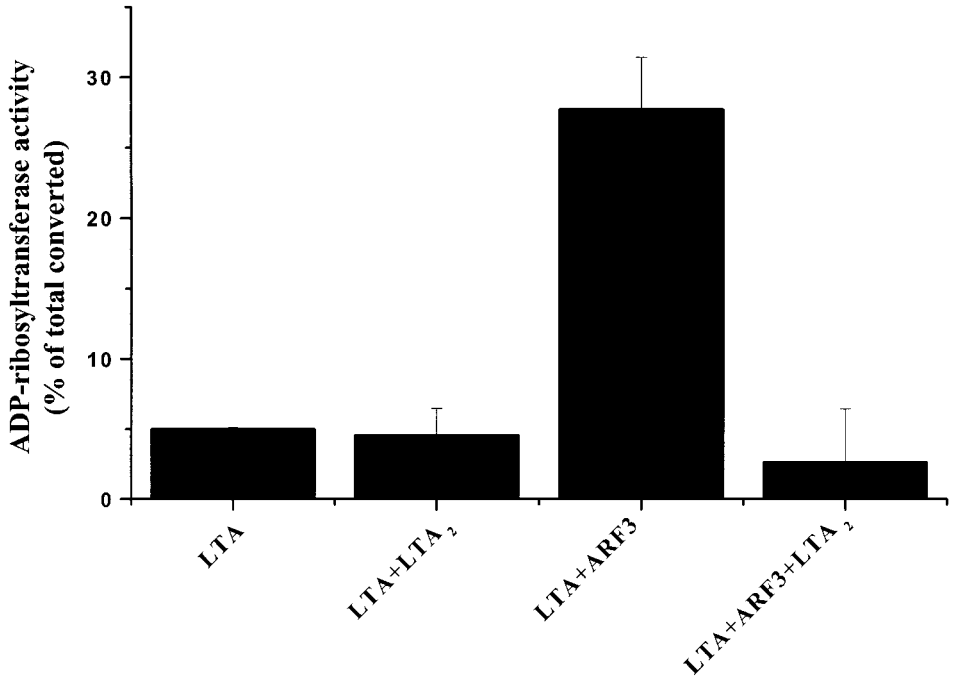

FIGURE 4: ARF-dependent, but not basal, ADP-ribosyltransferase activity of LTA was inhibited by the addition of excess LTA_2. LTA (120 μg) was activated by incubation at 30 °C for 10 min in buffer containing 50 mM glycine (pH 8.0), 20 mM dithiothreitol, and 2 μg of trypsin (type I from bovine pancreas) to ensure complete cleavage into subunits A_1 and A_2. The reaction was stopped with 12 μg of soybean trypsin inhibitor (type I-S). The ADP-ribosylation assays were performed for 90 min at 30 °C, as described in Materials and Methods. Reactions were initiated by the addition of activated LTA (final concentration of 2 μM) with or without added LTA_2 (18 μM) and ARF3 (2 μM). The averages of triplicate determinations are shown with error bars representing the standard error of the mean. This experiment was repeated at least twice.

LTA_1 and that the LTA_2 subunit and ARF share structural homology in this domain that confers upon LTA_2 the ability to bind to ARF effectors, i.e., a weak ARF-mimetic activity.

Our original observation was the similarity in the three-dimensional organization of α-helices between the surface of RAS GAP on which the GTPase binds with the flexible, catalytic loop and the C-terminal helices and flexible loop of LTA_1. Directed mutagenesis studies confirmed the importance of these regions in LTA_1 to ARF binding. This analogy was extended even further when it was found that the residue homologous to the catalytic Arg^{789} in RAS GAP was Arg^{33} in LTA_1 and that it is required for binding of ARF3 and LTA_1. Thus, the organization of α-helices and a flexible loop with a critical arginine may be a common motif found in GTPase binding proteins that is not just limited to providing an arginine for the purpose of coordinating the catalytic water in the GTPase reaction.

Four of the residues of LTA_1, identified in our studies as capable of influencing the binding of [Q71L]ARF3, are predicted from modeling of the holotoxin structure to make contact with the A_2 subunit. Structures of LT (*10*) reveal contacts between Phe^{31} with Val^{218} and Lys^{219} in LTA_2. And Arg^{33} in LTA_1 is oriented toward Gln^{215} in LTA_2. Asn^{93} and Tyr^{149} in LTA_1 make hydrophobic interactions with Tyr^{214} and Gln^{221} in LTA_2. The distances between the side chains of LTA_1 and LTA_2 in the structure of the holotoxin are in the range of 3.0−4.0 Å, though it is not known what these distances are in solution. Overall, our results reveal that ARF and the A_2 subunit bind to a largely overlapping region of the A_1 subunit. In contrast, mutation of Asp^{32} to histidine, in the same loop, had no effect on the binding to ARF, as it makes no contacts with the A_2 subunit and its side chain is facing away from the predicted binding surface. We interpret this as evidence that the binding of ARF involves at least two residues in the loop of residues 26−35 and that the orientation of residues 31 and 33 toward solvent that is found in the holotoxin is likely preserved in the ARF(GTP)·LTA complex.

Although it was not determined directly in these studies, we expect that the binding of LTA_2 to LTA_1 is of lower affinity than that of activated ARFs. We interpret the results in Table 4 as indicating that LTA_2 binds to LTA_1 through a series of side chain interactions such that loss of one does not result in a large change in binding. In contrast, ARFs interact with several of the same residues of LTA_1 but are predicted to make more intimate contacts with fewer key residues such that their loss reduces the level of binding dramatically.

The Trp^{174} to Ile^{174} mutation or truncation at Trp^{179} led to the loss of all detectible LTA activity (*37*). From our loss-of-interaction screen, we found that mutation of Trp^{179} to Arg was equally potent in disrupting the binding of [Q71L]-ARF3 and [E112D]LTA. This residue lies in a hydrophobic environment, named the third globular domain by Zhang et al. (*60*), rich in aromatic and hydrophobic residues, including a cluster of prolines and two tryptophans (Trp^{174} and Trp^{179}). Hydrophobic interactions are also observed between these prolines (Pro^{169} and Pro^{184}) and residues in the A_2 subunit (Gly^{196}, Cys^{199}, and Glu^{202}). Though no direct contact is observed between Trp^{179} and LTA_2, the mutation to an arginine is predicted to disrupt the overall hydrophobic environment around the interface between A_1 and A_2. The exact role of this hydrophobic region in the binding of ARF and activation of the ADP-ribosyltransferase activity must await more detailed structural analyses, e.g., from an ARF·LTA cocrystal.

The overall structure of the catalytic LTA_1 subunit is organized into three distinct domains (*10*, *60*). Mutation of Arg^7 caused increased flexibility of the loop of residues 25−36 and the active site loop of residues 47−56 (*38*). From these detailed structural observations, it was predicted that a sequence of conformational changes is required for full activation of LTA, and these conformational changes start from the C-terminal region of LTA_1 and propagate through the flexible loop (residues 25−36) to affect the active site loop (*38*). The other loop (residues 47−56) may be influenced indirectly, e.g., in response to changes in the loop of residues 25−36, as a helix-breaking mutation in the short α-helix immediately upstream of this loop (Asp^{43} → Gly) was sufficient to disrupt the binding of ARF. As our results point to the importance of the C-terminus and the finger loop of residues 25−36 to ARF binding, we predict that ARF stabilizes these conformational changes to produce a more active form of the toxin through the binding of the C-terminal region and the finger loop of LTA_1.

The LTA_2 subunit is a long α-helix with a KDEL motif at its C-terminus and making extensive contacts with the C-terminal region of the A_1 subunit through residues 195−220 and to the B pentamer through the rest of the residues (amino acids 220−236) (*10*). Of the at least 15 structures for LT in the protein database, all include the B pentamer so we do not yet have a high-resolution picture of LTA that is not influenced by the binding of the B subunits. This is most likely only important to those interactions nearer the C-terminus of LTA_2 in terms of the distances between the two LTA subunits. Despite this, the most extensive contacts are between Gln^{215} and Lys^{219} of LTA_2 and Phe^{31} and Arg^{33} of LTA_1. It is this very region of LTA_2 whose sequence is homologous to the switch II region of ARFs and led us to test for the ability of LTA_2 to bind other ARF effectors. Though switch I of GTPases has also been termed the "effector binding domain", a recent structure revealed that the switch II domain of ARF was involved in binding to the catalytic domain of an ARF GAP and suggested that switch I may be free to bind other proteins simultaneously (*31*). We found that the A_2 subunit contains a switch II-like motif and interacts weakly but specifically with the same ARF effectors that bind [Q71L]ARF3 in two-hybrid assays.

The use of cellular regulatory proteins as essential cofactors for bacterial toxins is an intriguing theme in the evolution of the relationship between pathogen and host that remains poorly understood. Several examples have now been found in which the hijacking of normal cellular processes by the pathogen or its toxin is used to evade host responses or access specific cellular domains or targets. The presence of a KDEL sequence at the C-terminus of LT and CT, to direct the retrograde transport of the toxins to the ER, is just one example. Perhaps the presence of an ARF-mimetic domain in the middle of the LTA_2 protein is another. Lencer et al. (*61*, *62*) summarize the evidence that the LTA subunit may be accessible to the cytosol, by partial translocation through the pore in the B pentamer. It is thus possible that this switch II-like domain of LTA_2 is available for interaction with ARF effectors and could direct the traffic of vesicles prior to the arrival of the toxin at the ER and later translocation across the membrane. These currently remain tantalizing possibilities that require additional tests but will likely provide insight into both the actions of the toxins and those of the protein cofactor.

ACKNOWLEDGMENT

We thank Lan Zhou for assistance in making the ribbon figure of the LTA structure, Wendy Smith-Oglesby for expert secretarial assistance, and Dr. Stephen J. Elledge for providing the original two-hybrid yeast strains and plasmids. We also thank all members of the Kahn laboratory for their help during the course of these studies.

REFERENCES

1. Kaper, J. B., Morris, J. G., Jr., and Levine, M. M. (1995) *Clin. Microbiol. Rev. 8*, 48−86.
2. de Haan, L., and Hirst, T. R. (2000) *J. Nat. Toxins 9*, 281−297.
3. Merritt, E. A., and Hol, W. G. (1995) *Curr. Opin. Struct. Biol. 5*, 165−171.
4. Merritt, E. A., Pronk, S. E., Sixma, T. K., Kalk, K. H., van Zanten, B. A., and Hol, W. G. (1994) *FEBS Lett. 337*, 88−92.
5. Sixma, T. K., Pronk, S. E., Kalk, K. H., Wartna, E. S., van Zanten, B. A., Witholt, B., and Hol, W. G. (1991) *Nature 351*, 371−377.
6. Streatfield, S. J., Sandkvist, M., Sixma, T. K., Bagdasarian, M., Hol, W. G., and Hirst, T. R. (1992) *Proc. Natl. Acad. Sci. U.S.A. 89*, 12140−12144.
7. Cassel, D., and Pfeuffer, T. (1978) *Proc. Natl. Acad. Sci. U.S.A. 75*, 2669−2673.
8. Gill, D. M., and Richardson, S. H. (1980) *J. Infect. Dis. 141*, 64−70.
9. Northup, J. K., Sternweis, P. C., Smigel, M. D., Schleifer, L. S., Ross, E. M., and Gilman, A. G. (1980) *Proc. Natl. Acad. Sci. U.S.A. 77*, 6516−6520.
10. Sixma, T. K., Kalk, K. H., van Zanten, B. A., Dauter, Z., Kingma, J., Witholt, B., and Hol, W. G. (1993) *J. Mol. Biol. 230*, 890−918.
11. Eidels, L., Proia, R. L., and Hart, D. A. (1983) *Microbiol. Rev. 47*, 596−620.
12. Gill, D. M. (1976) *Biochemistry 15*, 1242−1248.
13. Majoul, I. V., Bastiaens, P. I., and Soling, H. D. (1996) *J. Cell Biol. 133*, 777−789.
14. Rodighiero, C., Aman, A. T., Kenny, M. J., Moss, J., Lencer, W. I., and Hirst, T. R. (1999) *J. Biol. Chem. 274*, 3962−3969.
15. Kahn, R. A., and Gilman, A. G. (1984) *J. Biol. Chem. 259*, 6228−6234.
16. Schleifer, L. S., Kahn, R. A., Hanski, E., Northup, J. K., Sternweis, P. C., and Gilman, A. G. (1982) *J. Biol. Chem. 257*, 20−23.
17. Brown, H. A., Gutowski, S., Moomaw, C. R., Slaughter, C., and Sternweis, P. C. (1993) *Cell 75*, 1137−1144.
18. Cockcroft, S., Thomas, G. M., Fensome, A., Geny, B., Cunningham, E., Gout, I., Hiles, I., Totty, N. F., Truong, O., and Hsuan, J. J. (1994) *Science 263*, 523−526.
19. Godi, A., Pertile, P., Meyers, R., Marra, P., Di Tullio, G., Iurisci, C., Luini, A., Corda, D., and De Matteis, M. A. (1999) *Nat. Cell Biol. 1*, 280−287.
20. Honda, A., Nogami, M., Yokozeki, T., Yamazaki, M., Nakamura, H., Watanabe, H., Kawamoto, K., Nakayama, K., Morris, A. J., Frohman, M. A., and Kanaho, Y. (1999) *Cell 99*, 521−532.
21. Balch, W. E., Kahn, R. A., and Schwaninger, R. (1992) *J. Biol. Chem. 267*, 13053−13061.
22. Serafini, T., Orci, L., Amherdt, M., Brunner, M., Kahn, R. A., and Rothman, J. E. (1991) *Cell 67*, 239−253.
23. Orci, L., Palmer, D. J., Amherdt, M., and Rothman, J. E. (1993) *Nature 364*, 732−734.
24. Lenhard, J. M., Kahn, R. A., and Stahl, P. D. (1992) *J. Biol. Chem. 267*, 13047−13052.
25. Boman, A. L., Taylor, T. C., Melancon, P., and Wilson, K. L. (1992) *Nature 358*, 512−514.

26. Stamnes, M. A., and Rothman, J. E. (1993) *Cell 73*, 999−1005.
27. Faundez, V., Horng, J. T., and Kelly, R. B. (1997) *J. Cell Biol. 138*, 505−515.
28. Greasley, S. E., Jhoti, H., Teahan, C., Solari, R., Fensome, A., Thomas, G. M., Cockcroft, S., and Bax, B. (1995) *Nat. Struct. Biol. 2*, 797−806.
29. Amor, J. C., Harrison, D. H., Kahn, R. A., and Ringe, D. (1994) *Nature 372*, 704−708.
30. Goldberg, J. (1998) *Cell 95*, 237−248.
31. Goldberg, J. (1999) *Cell 96*, 893−902.
32. Zhu, X., Boman, A. L., Kuai, J., Cieplak, W., and Kahn, R. A. (2000) *J. Biol. Chem.* (in press).
33. Noda, M., Tsai, S. C., Adamik, R., Moss, J., and Vaughan, M. (1990) *Biochim. Biophys. Acta 1034*, 195−199.
34. Domenighini, M., Montecucco, C., Ripka, W. C., and Rappuoli, R. (1991) *Mol. Microbiol. 5*, 23−31.
35. Domenighini, M., Magagnoli, C., Pizza, M., and Rappuoli, R. (1994) *Mol. Microbiol. 14*, 41−50.
36. Domenighini, M., and Rappuoli, R. (1996) *Mol. Microbiol. 21*, 667−674.
37. Burnette, W. N., Kaslow, H. R., and Moss, J. (1995) *Adv. Exp. Med. Biol. 8*, 1513−1518.
38. van den Akker, F., Merritt, E. A., Pizza, M., Domenighini, M., Rappuoli, R., and Hol, W. G. (1995) *Biochemistry 34*, 10996−11004.
39. Scheffzek, K., Ahmadian, M. R., Kabsch, W., Wiesmuller, L., Lautwein, A., Schmitz, F., and Wittinghofer, A. (1997) *Science 277*, 333−338.
40. Elson, C. O., and Ealding, W. (1984) *J. Immunol. 132*, 2736−2741.
41. Clements, J. D., Hartzog, N. M., and Lyon, F. L. (1988) *Vaccine 6*, 269−277.
42. Lycke, N., Tsuji, T., and Holmgren, J. (1992) *Eur. J. Immunol. 22*, 2277−2281.
43. Nashar, T. O., Amin, T., Marcello, A., and Hirst, T. R. (1993) *Vaccine 11*, 235−240.
44. Durfee, T., Becherer, K., Chen, P. L., Yeh, S. H., Yang, Y., Kilburn, A. E., Lee, W. H., and Elledge, S. J. (1993) *Genes Dev. 7*, 555−569.
45. Boman, A., Kuai, J., Zhu, X., Chen, J., Kuriyama, R., and Kahn, R. (1999) *Cell Motil. Cytoskeleton 44*, 119−132.
46. Muhlrad, D., Hunter, R., and Parker, R. (1992) *Yeast 8*, 79−82.
47. Kuai, J., Boman, A., Arnold, R., Zhu, X., and Kahn, R. (2000) *J. Biol. Chem. 275*, 4022−4032.
48. Bai, C., and Elledge, S. J. (1996) *Methods Enzymol. 273*, 331−347.
49. Studier, F. W., Rosenberg, A. H., Dunn, J. J., and Dubendorff, J. W. (1990) *Methods Enzymol. 185*, 60−89.
50. Studier, F. W., and Moffatt, B. A. (1986) *J. Mol. Biol. 189*, 113−130.
51. Rosenberg, A. H., Lade, B. N., Chui, D. S., Lin, S. W., Dunn, J. J., and Studier, F. W. (1987) *Gene 56*, 125−135.
52. Kahn, R. A. (1991) *Methods Enzymol. 195*, 233−242.
53. Randazzo, P. A., Weiss, O., and Kahn, R. A. (1995) *Methods Enzymol. 257*, 128−135.
54. Guarente, L. (1983) *Methods Enzymol. 101*, 181−191.
55. Moss, J., Manganiello, V. C., and Vaughan, M. (1976) *Proc. Natl. Acad. Sci. U.S.A. 73*, 4424−4427.
56. Boman, A. L., Zhang, C. J., Zhu, X., and Kahn, R. A. (2000) *Mol. Biol. Cell* (in press).
57. Cieplak, W., Jr., Mead, D. J., Messer, R. J., and Grant, C. C. (1995) *J. Biol. Chem. 270*, 30545−30550.
58. Moss, J., Stanley, S. J., Vaughan, M., and Tsuji, T. (1993) *J. Biol. Chem. 268*, 6383−6387.
59. Lee, C. M., Chang, P. P., Tsai, S. C., Adamik, R., Price, S. R., Kunz, B. C., Moss, J., Twiddy, E. M., and Holmes, R. K. (1991) *J. Clin. Invest. 87*, 1780−1786.
60. Zhang, G. F., Patton, W. A., Lee, F. J., Liyanage, M., Han, J. S., Rhee, S. G., Moss, J., and Vaughan, M. (1995) *J. Biol. Chem. 270*, 21−24.
61. Lencer, W. I., de Almeida, J. B., Moe, S., Stow, J. L., Ausiello, D. A., and Madara, J. L. (1993) *J. Clin. Invest. 92*, 2941−2951.
62. Lencer, W. I., Hirst, T. R., and Holmes, R. K. (1999) *Biochim. Biophys. Acta 1450*, 177−190.

BI002628S